

Shadow of Schwarzschild Black Hole in the Cold Dark Matter Halo

Shi-Jie Ma, Tian-Chi Ma, Jian-Bo Deng, and Xian-Ru Hu*

Lanzhou Center for Theoretical Physics,

Key Laboratory of Theoretical Physics of Gansu Province,

Lanzhou University, Lanzhou, Gansu 730000, China

Abstract

The Schwarzschild black hole in the Cold Dark Matter (CDM) halo is studied, and the radiation laws of the thin accretion disk near the black hole are discussed and summarized. The orbits of light around the black hole are also calculated. Additionally, using the Novikov-Thorne model's light intensity function of the thin accretion disk, it is possible to solve for the shadow created by the thin accretion disk near the Schwarzschild black hole as well as the observed luminosity of the disk.

keywords: the CDM halo, Schwarzschild black hole; thin accretion disk.

PACS No.: 04.20.-q

* Email: huxianru@lzu.edu.cn

I. INTRODUCTION

Since Einstein established general relativity, it has explained and predicted many phenomena in cosmic research, leading to new developments in cosmology [1–4]. However, in recent years, a gravitational effect has been observed that cannot be explained without the presence of additional, invisible matter. To address this issue, cosmologists proposed the existence of dark matter, which is now believed to account for approximately 85 % of the universe [5–7]. Dark matter can't be easily observed because they may not participate in electromagnetic interaction. So we only could investigate these properties via these gravitational effect.

James Peebles first proposed the Cold Dark Matter (CDM) model in [8]. "Cold" means that dark matter moves slowly compared to the speed of light. The predictions of the CDM paradigm are basically consistent with the observation of the large-scale structure of the universe. Since the late 1980s or 1990s, most cosmologists prefer the CDM theory, especially the Λ CDM model [9, 10], to describe how the universe develops.

According to the model of modern physical cosmology, the dark matter halo is the basic unit of cosmic structure. The hypothesis for CDM structure formation begins with density perturbations in the Universe that grow linearly until they reach a critical density. After that, they stop expanding and collapse to form gravitationally bound dark matter halos [11]. The metric of black holes in dark matter has

been studied in recent years [12], this provides theoretical help for us to study the spherically symmetric black hole in the CDM halo.

The photon sphere, gravitational lens, black hole shadow, and other issues have received widespread attention, but we are particularly interested in black hole shadows [13–18], especially shadow produced by the thin accretion disk as the light source, because thin accretion disk is so bright. Thin accretion disk has been widely studied [19–39]. The Novikov-Thorne model was firstly proposed by ID Novikov and KS Thorne in 1973 to describe the thin accretion disk around the rotating black hole [22, 23]. Surely it doesn’t hinder us to use this model to research static black hole, like Schwarzschild black hole with thin accretion disk.

In order to gain a more comprehensive understanding of the appearance of black holes in the CDM halo, we will take the Schwarzschild black hole in the CDM halo as an example and conduct a comprehensive analysis of shadows, photon rings, and lensing rings. In Section II, we calculate the geodesic of the Schwarzschild black hole in the CDM halo. In Section III, we calculate the light orbit of the black hole, obtain the deflection angle of the light orbit under the influence of black hole gravity, and explore the influence of relevant parameters of the dark matter halo on the light orbit. In Section IV, we calculate the relationship between the observed light intensity of the observer at infinity and the light intensity of the light source near the black hole. In Section V, we use the light intensity distribution that conforms to the actual

luminous law to plot the observed intensities. Finally, in Section VI, we analyze the influence of the CDM halo parameter on the radiation mode. We provide a conclusion and outlook in Section VII. In this paper, to simplify the calculation, we assume $G_N = M = C = 1$.

II. GEODESIC EQUATIONS IN THE CDM HALO

In [12], we get the metric of Schwarzschild black hole in the CDM halo.

$$ds^2 = g_{\mu\nu} dx^\mu dx^\nu = -g(r) dt^2 + \frac{dr^2}{g(r)} + r^2 (d\theta^2 + \sin^2 \theta d\varphi^2), \quad (1)$$

where $g_{\mu\nu}$ is the covariant tensor of Riemann metric and

$$g(r) = \left(1 + \frac{r}{R_0}\right)^{-\frac{8\pi\rho_0 R_0^3}{r}} - \frac{2}{r}. \quad (2)$$

ρ_0 is the density of the CDM halo collapse, R_0 is the feature radius. It can be seen that when $\rho_0 = 0$ or $R_0 \rightarrow 0$, $g(r)$ will degenerate to $1 - 2/r$, so the metric will degenerate to Schwarzschild metric.

Under the arbitrary metric, the Lagrangian of the particle is given by

$$\mathcal{L} = \frac{1}{2} g_{\mu\nu} \dot{x}^\mu \dot{x}^\nu, \quad (3)$$

and the geodesic equation under any metric is

$$\frac{d\dot{x}^\sigma}{d\lambda} + \Gamma_{\mu\nu}^\sigma \dot{x}^\mu \dot{x}^\nu = 0, \quad (4)$$

where λ is affine parameter, $\dot{x}^\mu = \frac{dx^\mu}{d\lambda}$ are the four-velocities of the physical particle or the tangent wave vectors of the light and $\Gamma_{\mu\nu}^\sigma$ are Christoffel symbols, $\Gamma_{\mu\nu}^\sigma$ are given by

$$\Gamma_{\mu\nu}^\sigma = \frac{1}{2}g^{\sigma\delta}(\partial_\mu g_{\delta\nu} + \partial_\nu g_{\mu\delta} - \partial_\delta g_{\mu\nu}), \quad (5)$$

with $g^{\mu\nu}$ is the inverse tensor of Riemann metric.

For the static spherically symmetric metric, we can always limit the motion of particles on the equatorial plane, that is $\theta = \pi/2$ and $d\theta/ds = 0$, so we can get the following three equations:

$$\dot{t} = \frac{E}{g(r)}, \quad (6)$$

$$\dot{\varphi} = \frac{L}{r^2}, \quad (7)$$

$$\dot{r} = \sqrt{E^2 - g(r) \frac{L^2}{r^2} + 2\mathcal{L}g(r)}, \quad (8)$$

where E is energy and L is angular momentum, both of which are conserved quantities. Eliminate the affine parameter to get

$$\left(\frac{dr}{d\varphi}\right)^2 = r^4 \left(\frac{1}{b^2} - \frac{g(r)}{r^2} + \frac{2\mathcal{L}g(r)}{L^2}\right) = V_{eff} \quad (9)$$

where $b = L/E$ is called the impact parameter.

III. NULL GEODESIC AND THE TOTAL CHANGE OF AZIMUTHAL ANGLE

To understand the relationship between all light orbits and b , we substitute the null geodesic Lagrangian ($\mathcal{L} = 0$) into Eq. (9) and obtain:

$$\left(\frac{dr}{d\varphi}\right)^2 = r^4 \left(\frac{1}{b^2} - \frac{g(r)}{r^2}\right). \quad (10)$$

For simplicity in calculation, r is replaced with $u = 1/r$, the resulting orbital equation becomes

$$\left(\frac{du}{d\varphi}\right)^2 = G(u), \quad (11)$$

where

$$G(u) = \frac{1}{b^2} - u^2 \left(\left(1 + \frac{1}{uR_0}\right)^{-8\pi\rho_0 R_0^3 u} - 2u \right). \quad (12)$$

According to Eq. (11) and Eq. (12), we can calculate the total change of azimuthal angle φ for a certain orbit with impact parameter b as follows:

$$\varphi = \begin{cases} 2 \int_0^{u_m} \frac{du}{\sqrt{G(u)}} & b > b_c \\ \int_0^{u_0} \frac{du}{\sqrt{G(u)}} & b < b_c \end{cases}. \quad (13)$$

Here, b_c is the impact parameter corresponding to the circular orbit of light (i.e., photon sphere), and is also the shadow radius of the black hole. We can obtain b_c and the corresponding photon sphere radius r_c by setting $V_{eff} = V'_{eff} = 0$. At $b > b_c$, light will not fall into the black hole, and at $b < b_c$, light will fall into the black hole.

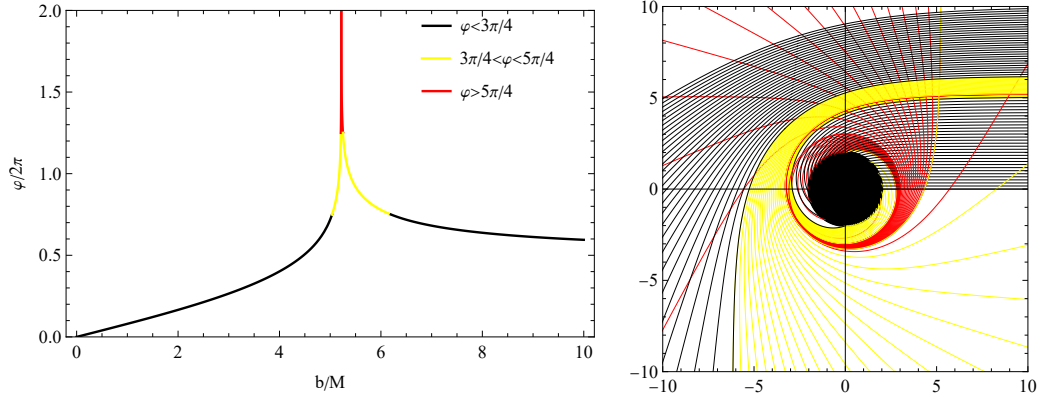


Figure 1: The relationship between φ and b (left) and the orbit of light near the black hole in the CDM halo(right). We set $\rho_0 = 0.1$, $R_0 = 0.1$. Different colors correspond to $\varphi < 3\pi/4$ (black), $3\pi/4 < \varphi < 5\pi/4$ (yellow) and $\varphi > 5\pi/4$ (red). On the right, we show the Euclidean polar coordinates (r, φ) . The settings of all orbit colors are the same as those in the left figure. The black hole is shown as a black disk in the middle of the image.

u_m is the turning point at $b > b_c$, corresponding to the minimum positive real root of $G(u) = 0$. $u_0 = 1/r_0$ corresponds to the radius of the event horizon.

We define $b_n^- < b_c$ and $b_n^+ > b_c$, where n is the number of times that light from infinity passes through the equatorial plane of the black hole. We use b_n^\pm to represent the solutions of the following equation.

$$\varphi(b) = \left(n - \frac{1}{2}\right) \pi, \quad n = 1, 2, 3 \dots \quad (14)$$

According to the number of times light passes through the equatorial plane, it can be

Table I: Various important physical parameters when $\rho_0 = 0.1$ and R_0 takes different values.

R_0	r_0	r_c	b_1^-	b_2^-	b_3^-	b_c	b_3^+	b_2^+
0	2	3	2.8477	5.0151	5.1878	5.1962	5.2279	6.1678
0.1	2.0076	3.0117	2.8588	5.0363	5.2102	5.2156	5.2506	6.1965
0.2	2.0481	3.0740	2.9181	5.1515	5.3321	5.3409	5.3746	6.3575
0.3	2.1375	3.2125	3.0498	5.4125	5.6096	5.6197	5.6574	6.7322

Table II: Various important physical parameters when $R_0 = 0.1$ and ρ_0 takes different values.

ρ_0	r_0	r_c	b_1^-	b_2^-	b_3^-	b_c	b_3^+	b_2^+
0	2	3	2.8477	5.0151	5.1878	5.1962	5.2279	6.1678
0.1	2.0076	3.0117	2.8588	5.0363	5.2102	5.2156	5.2506	6.1965
0.2	2.0153	3.0234	2.8700	5.0575	5.2325	5.2409	5.2733	6.2254
0.3	2.0229	3.0351	2.8811	5.0787	5.2548	5.2634	5.2959	6.2543

divided into direct orbit ($n = 1$), lended orbit ($n = 2$) and photo ring orbit ($n \geq 3$).

The physical picture of this classification is clear from the orbit plots in Fig. 1. Assuming that the light is emitted from the north pole (the rightmost side of the

plot). When $b \rightarrow \infty$, the azimuth of light around the black hole changes to $\varphi \rightarrow \pi/2$, so there is no corresponding b_1^+ .

We tried to calculate r_0 , r_c , b_c , b_1^- , b_2^\pm and b_3^\pm for different ρ_0 and R_0 , and wrote them in Table I and Table II.

Table I displays various important physical parameters for different values of R_0 when $\rho_0 = 0.1$. Table II displays various important physical parameters for different values of ρ_0 when $R_0 = 0.1$.

Table I presents various important physical parameters for different values of R_0 , when $\rho_0 = 0.1$. From the table, it is evident that all the parameters increase with an increase in R_0 , while ρ_0 remains constant. Similarly, Table II shows various important physical parameters for different values of ρ_0 , when $R_0 = 0.1$. The table reveals that all the parameters increase with an increase in ρ_0 , while R_0 remains constant. These results suggest that light observed from different regions will be farther away from the center of the black hole as ρ_0 and R_0 increase. Additionally, Table I and Table II reveal that when $\rho_0 = 0$ and $R_0 \rightarrow 0$, the black hole degenerates to a Schwarzschild black hole in a vacuum and its parameters reach a minimum.

IV. OBSERVED SPECIFIC INTENSITIES AND TRANSFER FUNCTIONS

In general, the term 'shadow' describes how a black hole appears when illuminated from all directions. In sections II and III, we have explored the optical orbits near

the black hole in the CDM halo. Now, we are ready to consider a thin accretion disk on the equatorial plane around the black hole in the CDM halo. For an observer at infinity, what is observed is more important than the distribution of light intensity.

Now a simple example of a thin accretion disk around a black hole is considered, in which the radiation intensity depends only on the radial coordinates and absorption of light is neglected. We assume that the disk is isotropic within the stationary frame of the object on the stationary world line. This example serves as a model to illustrate the gravitational lensing and gravitational redshift effects. The disk is placed on the equatorial plane and we assume that the observer is located at the North Pole. $I_{\nu_e}^{em}(r)$ is used to express the specific intensity of emission. ν_e is the transmission frequency in the stationary coordinate system. The relative intensity of the light that an observer at infinity will receive is $I_{\nu_o}^{obs}$, ν_o is the frequency observed by the observer at infinity of the stationary reference system, and the frequency redshift is caused by the gravitational effect $\nu_o = \sqrt{g(r)}\nu_e$ [40]. Considering that there is a conserved quantity I_ν/ν^3 for a light [41], one can get

$$\frac{I_{\nu_o}^{obs}}{\nu_o^3} = \frac{I_{\nu_e}^{em}}{\nu_e^3}, \quad (15)$$

so the relative intensity we observed is

$$I_{\nu_o}^{obs} = \left(\frac{\nu_o}{\nu_e}\right)^3 I_{\nu_e}^{em}(r) = g^{3/2}(r) I_{\nu_e}^{em}(r). \quad (16)$$

The total intensity observed is an integral of all frequencies

$$I^{obs} = \int I_{\nu_o}^{obs} d\nu_o = \int g^2(r) I_{\nu_e}^{em}(r) d\nu_e = g^2(r) I^{em}(r), \quad (17)$$

where $I^{em}(r) = \int I_{\nu_e}^{em}(r) d\nu$ is the total emission intensity at the accretion disk at r .

Due to the high intensity of light emitted from the accretion disk, other light sources in the environment can be ignored. If a beam of light from the observer intersects with the emission disk, it means that the intersection point will contribute to the observed brightness as a light source. As mentioned in Section III, a light ray may pass through the equatorial plane of the black hole multiple times, and each intersection with the disk will become a light source contributing to the observed intensity for that orbit. Therefore, the observed intensity is the sum of the intensities of each intersection.

$$I^{obs}(b) = \sum_n g^2(r_n(b)) I^{em}, \quad (18)$$

where $r_n(b)$ is the so-called transfer function, which represents the radial position of the n -th intersection and the transmitting disk, that is, the radial coordinates of the luminous point. It should be emphasized that our model does not take into account the absorption and reflection of light by the accretion disk or the loss of light intensity in the environment, and is only an idealized representation.

We denote the solution of orbit Eq. (16) by $u(b, \varphi)$, so we can get the transfer

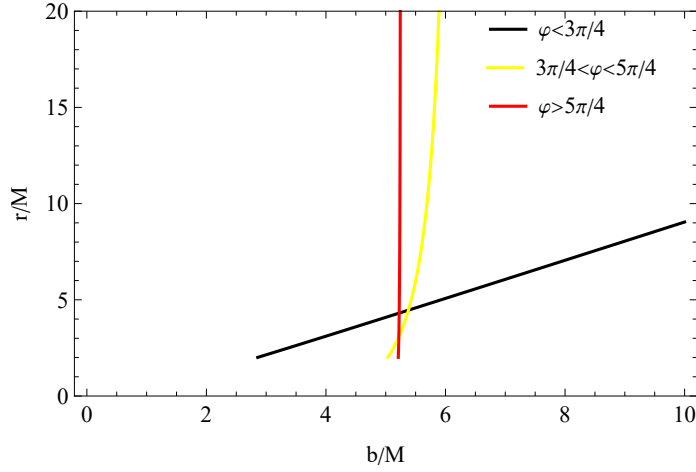


Figure 2: The first three transfer functions of black holes in the CDM halo with $\rho_0 = 0.1$, $R_0 = 0.1$. The three curves in the figure represent the radial coordinates of the first (black), second (yellow) and third (red) intersections with the accretion disk.

functions:

$$r_n(b) = \frac{1}{u\left(b, \frac{(2n-1)\pi}{2}\right)} \quad b \in (b_n^-, b_n^+), \quad (19)$$

here we take positive infinity as b_1^+ . In Fig. 2, we show the first three transfer functions of the black hole in the CDM halo.

V. RADIATION FROM STABLE CIRCULAR ORBIT

The model of thin accretion disk used in this paper meets the Novikov-Thorne model. According to assumptions of Novikov-Thorne model, the model conforms

to conservation laws of energy $(\nabla_\mu T^{t\mu})$, angular momentum $(\nabla_\mu T^{\varphi\mu})$, rest mass $(\nabla_\mu (\rho u^\mu))$ of particles in an accretion disk. By using these conservation laws, one can obtain the radiant energy flux as [22, 23]

$$F(r) = -\frac{\mathcal{M}\Omega'}{4\pi\sqrt{-g}(E-\Omega L)^2} \int_{r_{ISCO}}^r (E-\Omega L) L' dr, \quad (20)$$

where \mathcal{M} is the mass accretion rate, g is the determinant of metric tensor, r_{ISCO} is the radius of the innermost stable circular orbit (ISCO) of physical particles around a black hole ($2\mathcal{L} = -1$). The ISCO should satisfy $V_{eff} = V'_{eff} = V''_{eff} = 0$. There is a relation $A' = \frac{dA}{dr}$ for any physical quantity A . $\Omega = d\varphi/dt$ is angular velocity of particles in any stable circular orbits ($\dot{r} = \ddot{r} = 0$), for any stable circular orbit, there are

$$\begin{aligned} \Omega &= \sqrt{-\frac{g'_{tt}}{g'_{\varphi\varphi}}} \\ E &= -\frac{g_{tt}}{\sqrt{-g_{tt} - g_{\varphi\varphi}\Omega^2}} \\ L &= \frac{g_{\varphi\varphi}\Omega}{\sqrt{-g_{tt} - g_{\varphi\varphi}\Omega^2}} \end{aligned} \quad (21)$$

It is evident from Fig. 3 that the light intensity distribution observed by an observer at infinity is composed of several intensity peaks with the same shape but different widths, and most of the observed light intensity is contributed by $r = r_1(b)$. Although only $n = 3$ is calculated, the width of the corresponding peak narrows with the increase of n . As n becomes larger, the intensity peaks become less significant and can be ignored.

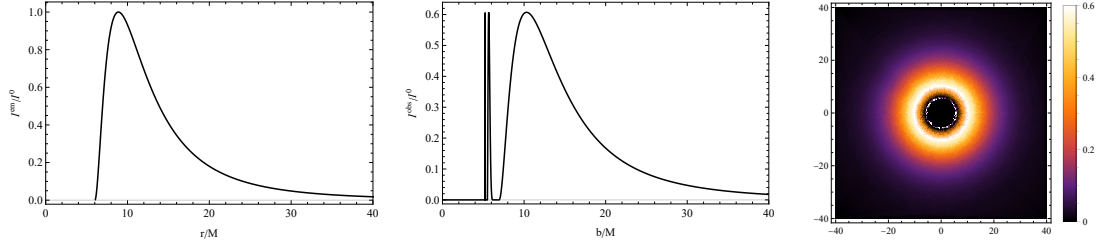


Figure 3: Emission specific intensity diagram (left), observation specific intensity diagram (middle) and halo diagram (right) of model given by Eq. (20) with

$$R_0 = 0.1 \text{ and } \rho_0 = 0.1.$$

VI. RADIATION FLUX AND OBSERVED LUMINOSITY

To understand the properties of the thin accretion disk near the Schwarzschild black hole in the CDM halo, the radiation flux and observed luminosity of the above radiation under different parameters have been calculated and analyzed.

In addition, we have also calculated the energy flux while keeping the mass accretion rate constant and varying the other parameters, and the results are presented in Fig. 4. As R_0 or ρ_0 increases, the peak value and total energy flux decrease, and the radii of the corresponding peaks increase.

Assuming that the accretion disk in this model is in local thermal equilibrium, we can assume that the radiation from the accretion disk is blackbody radiation. The

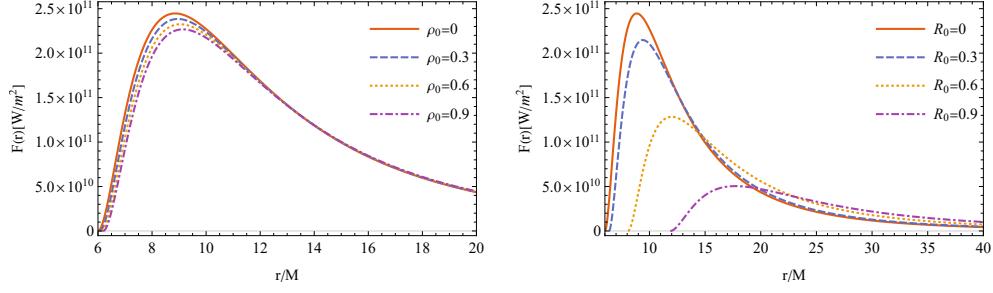


Figure 4: The energy flux $F(r)$ of an accretion disk around the black hole in CDM halo with mass accretion rate $\mathcal{M} = 2 * 10^{17} \text{ kg/s} \approx 3.2 * 10^{-6} m_{\text{sun}}/\text{year}$, for different values of the parameter ρ_0 with $R_0 = 0.1$ (left) and for different values of R_0 with $\rho_0 = 0.1$ (right).

observed luminosity of thin disks is given by [42]

$$\tilde{L}(\nu_o) = 8\pi h \cos \gamma \int_{r_{in}}^{r_{out}} \int_0^{2\pi} \frac{\nu_e^3 r dr d\varphi}{e^{\frac{h\nu_e}{k_B T}} - 1}, \quad (22)$$

where h is the Planck constant, k_B is the Boltzmann constant, γ is the disk inclination angle which we will set to zero. We will set $r_{in} = r_{ISCO}$, and r_{out} is the outer edge of the disk, it takes as $50 r_0$ [42]. T is the temperature of the disk, one can get by the Stefan-Boltzmann law

$$F(r) = \sigma T^4(r), \quad (23)$$

where σ is the Stefan-Boltzmann constant.

As shown in Fig. 5, with the increase of ρ_0 or R_0 , the accretion disk will become

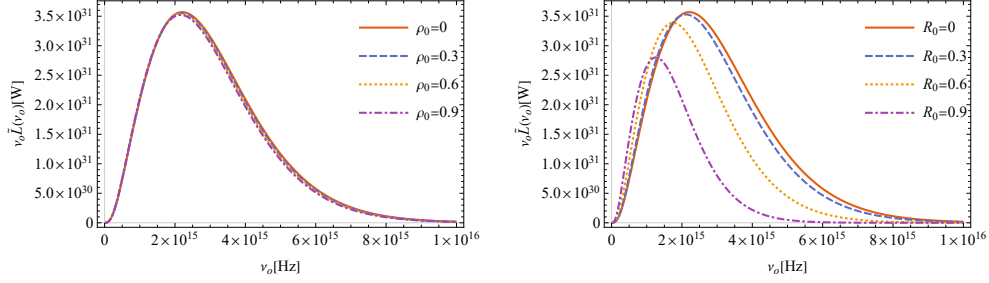


Figure 5: The emission spectrum $\nu_o \tilde{L}(\nu_o)$ of an accretion disk around the black hole in CDM halo with mass accretion rate $\mathcal{M} = 2 * 10^{17} kg/s$, for different values of the parameter ρ_0 with $R_0 = 0.1$ (left) and for different values of R_0 with $\rho_0 = 0.1$ (right).

dimmer, which is consistent with the previous analysis, and the cut-off frequency of the maximum luminosity moves to a lower value.

VII. CONCLUSION AND OUTLOOK

First, we calculate the geodesic equation of the Schwarzschild black hole in the CDM halo and the deflection angle of the photon orbit. We also analyze the relationship between the halo radius and the CDM halo parameters. Next, we calculate the relationship between the light intensity emitted by the thin accretion disk and the observed light intensity of the observer, as well as the transfer function. The metric used in this paper conforms to the Novikov-Thorne model, and we derive

the radiant energy flux according to the model. We plot the observed intensities of the radiation in the CDM halo and calculate the variation of the radiation flux and observed luminosity with the CDM halo parameters.

Looking to the future, there are two potential directions for further research. Firstly, we could investigate the radiation of accretion disks in other dark matter models and black hole models to gain a more comprehensive understanding of the behavior of thin disks in different astrophysical contexts. Secondly, recent research [43] has discovered a new shadow in a symmetrical thin-shell wormhole connecting two different vacuum Schwarzschild spacetimes. Similarly, it is possible that a new shadow may exist in a symmetrical thin-shell wormhole connecting two different Schwarzschild spacetimes in the case of the CDM halo. Therefore, it would be worthwhile to investigate the possibility of such a new shadow when considering the influence of the CDM halo.

CONFLICTS OF INTEREST

The authors declare that there are no conflicts of interest regarding the publication of this paper.

ACKNOWLEDGMENTS

We would like to thank the National Natural Science Foundation of China (Grant No.11571342) for supporting us on this work.

REFERENCES

- [1] Albert Einstein. Die feldgleichungen der gravitation. *Sitzung der physikalisch-mathematischen Klasse*, 25:844–847, 1915.
- [2] Albert Einstein. Näherungsweise integration der feldgleichungen der gravitation. *Sitzungsberichte der Königlich Preussischen Akademie der Wissenschaften*, pages 688–696, 1916.
- [3] Albert Einstein. Kosmologische betrachtungen zur allgemeinen relativitätstheorie. *Sitzungsberichte der Königlich Preussischen Akademie der Wissenschaften*, pages 142–152, 1917.
- [4] Hans C Ohanian and Remo Ruffini. *Gravitation and spacetime*. Cambridge University Press, 2013.
- [5] Seven-Year Wilson Microwave Anisotropy Probe. Observations: Sky maps, systematic errors, and basic results. nasa. gov. Technical report, Retrieved 2010-12-02.

- [6] Sean M Carroll. *Dark Matter, Dark Energy: The Dark Side of the Universe. Parts 1 & 2*. Teaching Company, 2007.
- [7] Fritz Zwicky. Die rotverschiebung von extragalaktischen nebeln. *Helvetica physica acta*, 6:110–127, 1933.
- [8] PJE Peebles. Large-scale background temperature and mass fluctuations due to scale-invariant primeval perturbations. *Astrophysical Journal, Letters to the Editor*, 263(1):L1–L5, 1982.
- [9] John Michael Kovac, EM Leitch, Clement Pryke, JE Carlstrom, NW Halverson, and WL Holzzapfel. Detection of polarization in the cosmic microwave background using dasi. *Nature*, 420(6917):772–787, 2002.
- [10] Peter AR Ade, N Aghanim, M Arnaud, Mark Ashdown, J Aumont, C Baccigalupi, AJ Banday, RB Barreiro, JG Bartlett, N Bartolo, et al. Planck 2015 results-xiii. cosmological parameters. *Astronomy & Astrophysics*, 594:A13, 2016.
- [11] Houjun Mo, Frank Van den Bosch, and Simon White. *Galaxy formation and evolution*. Cambridge University Press, 2010.
- [12] Zhaoyi Xu, Xian Hou, Xiaobo Gong, and Jiancheng Wang. Black hole space-time in dark matter halo. *Journal of Cosmology and Astroparticle Physics*, 2018(09):038, 2018.

- [13] Clarissa-Marie Claudel, K. S. Virbhadra, and G. F. R. Ellis. The Geometry of photon surfaces. *J. Math. Phys.*, 42:818–838, 2001.
- [14] K. S. Virbhadra. Distortions of images of Schwarzschild lensing. 4 2022.
- [15] K. S. Virbhadra. Compactness of supermassive dark objects at galactic centers. 4 2022.
- [16] Ali Övgün, İzzet Sakallı, Joel Saavedra, and Carlos Leiva. Shadow cast of noncommutative black holes in rastall gravity. *Modern Physics Letters A*, 35(20):2050163, 2020.
- [17] Ali Övgün, İzzet Sakallı, and Joel Saavedra. Shadow cast and deflection angle of kerr-newman-kasuya spacetime. *Journal of Cosmology and Astroparticle Physics*, 2018(10):041, 2018.
- [18] Sérgio VMCB Xavier, Haroldo CD Lima Junior, and Luís CB Crispino. Shadows of black holes with dark matter halo. *Physical Review D*, 107(6):064040, 2023.
- [19] NI Shakura. Critical luminosity for accretion and shell energy sources. *Soviet Astronomy*, 18:259, 1974.
- [20] R. A. Sunyaev. Accretion of matter onto black holes. *Symposium - International Astronomical Union*, 64:193–193, 1974.
- [21] Ni I Shakura and Rashid Alievich Sunyaev. Black holes in binary systems. observational appearance. *Astronomy and Astrophysics*, 24:337–355, 1973.

- [22] ID Novikov and KS Thorne. Black holes, edited by c. dewitt and bs dewitt, 1973.
- [23] Don N Page and Kip S Thorne. Disk-accretion onto a black hole. time-averaged structure of accretion disk. *The Astrophysical Journal*, 191:499–506, 1974.
- [24] MA Abramowicz and PC Fragile. Living rev. rel. 16, 1 (2013). *arXiv preprint arXiv:1104.5499*.
- [25] Sobhan Kazempour, Yuan-Chuan Zou, and Amin Rezaei Akbarieh. Analysis of accretion disk around a black hole in drgt massive gravity. *The European Physical Journal C*, 82(3):1–9, 2022.
- [26] Cheng Liu, Sen Yang, Qiang Wu, and Tao Zhu. Thin accretion disk onto slowly rotating black holes in einstein-æther theory. *Journal of Cosmology and Astroparticle Physics*, 2022(02):034, 2022.
- [27] Tong-Yu He, Rong-Jia Yang, and Ziqiang Cai. Accretion disk around a black hole in einstein-aether-scalar theory. *arXiv preprint arXiv:2208.03723*, 2022.
- [28] Kuantay Boshkayev, Talgar Konysbayev, Ergali Kurmanov, Orlando Luongo, Daniele Malafarina, and Hernando Quevedo. Luminosity of accretion disks in compact objects with a quadrupole. *Physical Review D*, 104(8):084009, 2021.
- [29] Galin Gyulchev, Petya Nedkova, Tsvetan Vetsov, and Stoytcho Yazadjiev. Image of the thin accretion disk around compact objects in the einstein–gauss–bonnet gravity. *The European Physical Journal C*, 81(10):1–10, 2021.

- [30] Mohaddese Heydari-Fard, Malihe Heydari-Fard, and Hamid Reza Sepangi. Thin accretion disks around rotating black holes in 4d einstein–gauss–bonnet gravity. *The European Physical Journal C*, 81(5):1–11, 2021.
- [31] Mohaddese Heydari-Fard and Hamid Reza Sepangi. Thin accretion disk signatures of scalarized black holes in einstein-scalar-gauss-bonnet gravity. *Physics Letters B*, 816:136276, 2021.
- [32] Zelin Zhang, Songbai Chen, Xin Qin, and Jiliang Jing. Polarized image of a schwarzschild black hole with a thin accretion disk as photon couples to weyl tensor. *The European Physical Journal C*, 81(11):1–10, 2021.
- [33] Cheng Liu, Tao Zhu, and Qiang Wu. Thin accretion disk around a four-dimensional einstein-gauss-bonnet black hole. *Chinese Physics C*, 45(1):015105, 2021.
- [34] R Kh Karimov, RN Izmailov, AA Potapov, and KK Nandi. Can accretion properties distinguish between a naked singularity, wormhole and black hole? *The European Physical Journal C*, 80(12):1–17, 2020.
- [35] Mohaddese Heydari-Fard, Malihe Heydari-Fard, and Hamid Reza Sepangi. Thin accretion disks and charged rotating dilaton black holes. *The European Physical Journal C*, 80(4):1–10, 2020.
- [36] Daniela Pérez, Federico G Lopez Armengol, and Gustavo E Romero. Accretion disks around black holes in scalar-tensor-vector gravity. *Physical Review D*, 95(10):104047,

2017.

- [37] Daniela Pérez, Gustavo E Romero, and SE Perez Bergliaffa. Accretion disks around black holes in modified strong gravity. *Astronomy & Astrophysics*, 551:A4, 2013.
- [38] Songbai Chen and Jiliang Jing. Properties of a thin accretion disk around a rotating non-kerr black hole. *Physics Letters B*, 711(1):81–87, 2012.
- [39] Songbai Chen and Jiliang Jing. Thin accretion disk around a kaluza–klein black hole with squashed horizons. *Physics Letters B*, 704(5):641–645, 2011.
- [40] CA Chant. Notes and queries (telescopes and observatory equipment-the einstein shift of solar lines). *Journal of the Royal Astronomical Society of Canada*, 24:390, 1930.
- [41] George B Rybicki and Benjamin C Bromley. Emission line formation in a relativistic accretion disk. *arXiv preprint astro-ph/9711104*, 1997.
- [42] Diego F Torres. Accretion disc onto a static non-baryonic compact object. *Nuclear Physics B*, 626(1-2):377–394, 2002.
- [43] Xiaobao Wang, Peng-Cheng Li, Cheng-Yong Zhang, and Minyong Guo. Novel shadows from the asymmetric thin-shell wormhole. *Physics Letters B*, 811:135930, 2020.